Numerical verification of a dual system's seismic response

Marios C. Phocas* and Tonia Sophocleous

Department of Architecture, Faculty of Engineering, University of Cyprus
75 Kallipoleos Str., P.O.Box 20537, 1678 Nicosia, Cyprus

Abstract. Structural control through integration of passive damping devices within the building structure has been increasingly implemented internationally in the last years and has proven to be a most promising strategy for earthquake safety. In the present paper an alternative configuration of an innovative energy dissipation mechanism that consists of slender tension only bracing members with closed loop and a hysteretic damper is investigated in its dynamic behavior. The implementation of the adaptable dual control system, ADCS, in frame structures enables a dual function of the component members, leading to two practically uncoupled systems, i.e., the primary frame, responsible for the normal vertical and horizontal forces and the closed bracing-damper mechanism, for the earthquake forces and the necessary energy dissipation. Three representative international earthquake motions of differing frequency contents, duration and peak ground acceleration have been considered for the numerical verification of the effectiveness and properties of the SDOF systems with the proposed ADCS-configuration. The control mechanism may result in significant energy dissipation, when the geometrical and mechanical properties, i.e., stiffness and yield force of the integrated damper, are predefined. An optimum damper ratio, *DR*, defined as the ratio of the stiffness to the yield force of the hysteretic damper, is proposed to be used along with the stiffness factor of the damper's- to the primary frame's stiffness, in order for the control mechanism to achieve high energy dissipation and at the same time to prevent any increase of the system's maximum base shear and relative displacements. The results are summarized in a preliminary design methodology for ADCS.

Keywords: structural control; energy dissipation; dual system

1. Introduction

Buildings subjected to strong horizontal forces originating from earthquake excitations have in their design an additional complexity, in avoiding significant permanent damage that may lead to local or global collapse. The structural building design concentrates in the development of adaptable structures with predefined secondary areas that may absorb and dissipate large amounts of the earthquake input energy through enhanced elasto-plastic deformations. A promising strategy in this field for avoiding severe structural damages is the transformation of the horizontal load bearing structures into kinetic mechanisms through the integration of damping devices (Housner *et al.* 1997, Martelli 2007, Symans *et al.* 2008, Lavan and Levy 2010). Passive metallic yielding-, friction,

---

*Corresponding author, Associate Professor, E-mail: mcphocas@ucy.ac.cy

viscoelastic and viscous devices have been developed for this purpose. As far as plastic hysteretic dampers are concerned, especially ADAS and TADAS are well known examples, developed for both, new seismic resisting designs and retrofit of frame structures (Dargush and Soong 1995, Di Sarno *et al.* 2005). In principle steel plate dampers attached to diagonals are added within moment resisting frames. A stable energy dissipation behavior of the systems could be verified in experimental tests and real applications (Tsai *et al.* 1993, Symans *et al.* 2008). Further developments concentrate in the optimization of the steel plates' section for improved energy dissipation behavior and at the same time easy manufacture. In this frame single round-hole- and double X-shaped steel dampers have been experimentally investigated by Li and Li (2007), whereas Ghabraie *et al.* (2010) developed numerically optimized shapes of steel slit plates, as originally proposed by Chan and Albermani (2008). In all cases the bracing components used for the integration of the damping devices, increase the overall stiffness of the system, as they consist of steel members stressed in compression, tension and bending. In addition the application of the members under compression leads to a relatively inefficient behavior of the system under cyclic loading; in every half-loading cycle the compression diagonal buckles and it therefore cannot participate in the energy dissipation process.

On the other side slender tension members such as cables have found up to date limited applications for the realization of the bracing's components (Di Sarno *et al.* 2005), primarily due to their tendency of becoming slack under tension yielding and compression buckling. A possible configuration solution in this aspect goes back with the development of a refined computer model for the Pall-March friction mechanism with slender cross braces (Filiautrault and Cherry 1988). During the dynamic excitation the rectangular damper deforms into a parallelogram, dissipating energy at the bolted joints through sliding friction and at the same time preventing the diagonals to buckle under compression. An actual implementation of cable members with inverted *V*-configuration in connection with a friction damper consisting of three rotating plates and circular friction pad discs placed in between is described in Mualla and Belev (2002).

An articulated quadrilateral of steel hysteretic dissipaters, *AQ*, with cross cables has been proposed by Renzi *et al.* (2007). Under significant deformations of the frame, *AQ* keeps all tendons in tension. The energy dissipation is based on the elasto-plastic flexure of steel plates with varying depth. A further light-weight system with bracing tension members and a hysteretic damper is developed by Kurata, DesRoches and Leon (2008). The system is composed of eight elastic cables and a central energy dissipater working with cyclic bending of two rigid elements interconnected through a rotational spring. In the cases of hysteretic dampers with cable bracings the energy dissipation performance of the system depends on the characteristic design of the damper's section.

Adaptable dual control systems, ADCS, as these have been originally proposed by Phocas and Pocanschi (2003), consist of a cable bracing with closed loop and a hysteretic damper of steel plates. The control mechanism is only responsible for the earthquake forces and the necessary energy dissipation, enabling the elastic response of the primary frame under static- (gravity and equivalent static wind loading) and dynamic loading (moderate, extremely irregular base excitations). The present analysis refers to an alternative ADCS-configuration, whereas the bracing forms with three cables a triangular shape, leaving major part in the elevation layout of the structure free for minimum interference in architectural terms. Certain aspects in respect to the configuration and the mechanical properties of the integrated bracing-damper mechanism were presented in Phocas and Sophocleous (2011) and Sophocleous and Phocas (2011). The present work comprises a numerical verification of the effectiveness and properties of the ADCS-technique for a SDOF

system. The dynamic behavior of a SDOF-model is analyzed in the time-history range based on three selected international strong ground motions with different frequency contents. Through the analysis predominant parameters characterizing ADCS seismic behavior are derived in respect to the geometrical and mechanical properties of the members, i.e., the damper's elastic stiffness and yield force. ADCS design recommendations given in the last part of the paper, aim at highest possible energy dissipation by the hysteretic damper without increase of the maximum base shear and relative displacements of the controlled system compared to the primary frame's responses.

2. Design configuration

ADCS consists of a cable bracing with closed loop and a hysteretic damper of steel plates. ADCS kinetic mechanism is based on a prototype connections design for the bracing members, realized with rotating discs. The cables are connected at the bottom of the column and are free to move horizontally and vertically at both joints of the frame, Fig. 1. At the frame's joint, on the side of the column base connection, the cables are interconnected through a rotating circular shaped disc, at the opposite frame's joint, through a rotating U-shaped disc that is linked to the frame's joint through a secondary diagonal cable. A hysteretic damper is placed perpendicularly, between the secondary bracing member and gusset plates welded to the column. The hysteretic damper consists of a series of triangular shaped steel plates, welded on two horizontal plates, Fig. 2. The plates´ characteristic shape enables uniform bending curvatures over the sections height. Therefore all section lines reach their maximum yielding potential at the same time under the developed shear forces.

The kinetic mechanism is activated during the seismic excitation by the horizontally induced motion at the base of the structure. In every half-loading cycle the respective displacement of the primary frame is followed by the cables through rotations of the eccentric discs. As shown in Fig. 3, for either sense of lateral displacement the discs rotate. The rotation results to respective axial displacements of the connection joints to the cables, stretching the members. Since the bracing members form a closed polygon, ideally the reactions on the primary frame are neutralized and the members remain under tension. When the system moves to the opposite direction, one of the two main diagonal cables goes into tension, while the other one tends to be subjected to compression.
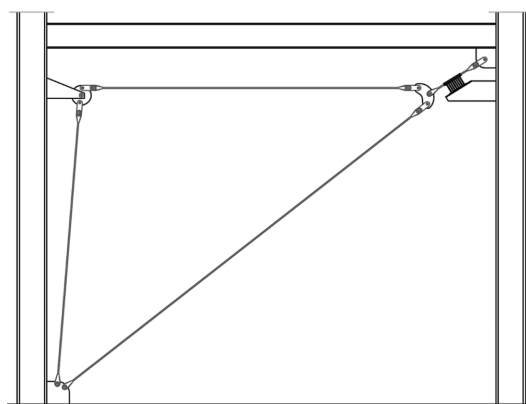

Fig. 1 Adaptable dual control system with cable bracing-damper mechanism
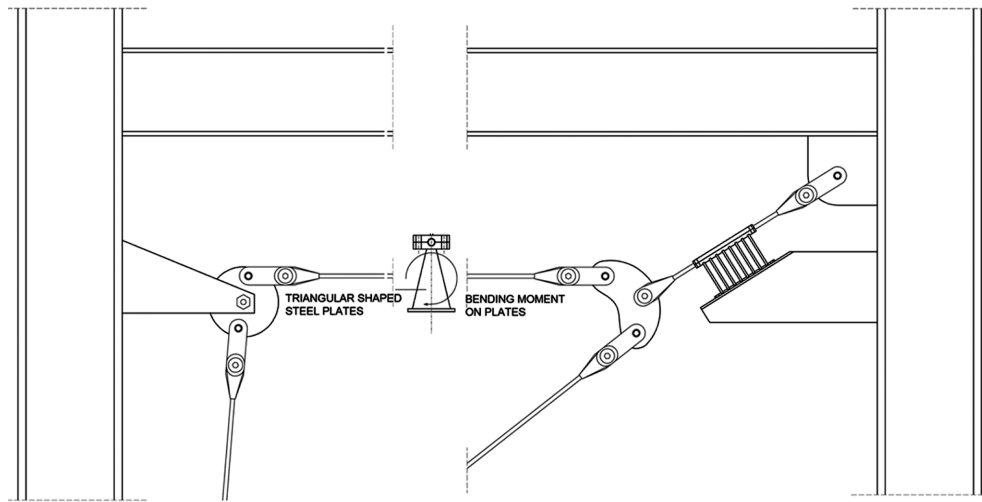
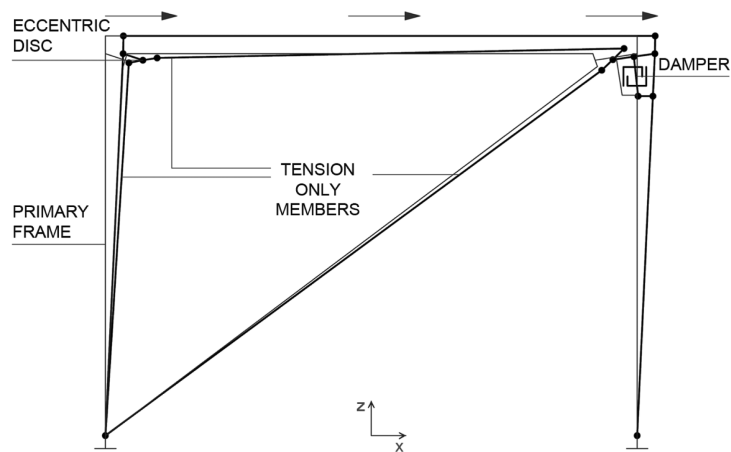Fig. 2 Connection principle of rotating discs and damper

Fig. 3 Kinetic system's model

Due to the closed loop arrangement, the tensioned cable stretches through the rotating disc the other one. In any case the rotating discs and the prestress of the cables ensure a smooth transition of forces in the tension-only members in each half-loading cycle change. Relative displacements between the secondary bracing member and the column lead to yielding deformations of the damper's steel plates for the necessary energy dissipation, Fig. 3. Thus the control concept of ADCS is based on achieving predefined performance levels through the property of deformation, rather than stiffness.

3. System model

ADCS dynamic analysis is based on a simplified SDOF model, whereas non-linearity is only

addressed to the hysteretic damper. ADCS was examined with the software program SAP2000. A typical geometry was assigned for the ideal 2D-model of a steel moment resisting frame with 4.5 m axis height and 6.0 m -length and loading characteristics of 1200 kN vertical load, 15 kN horizontal wind load and 25% of the vertical load as static equivalent seismic load. The columns consist of IPBv500 sections and the beams of an IPBL550 section ($S235$, $E = 2.1 \times 10^4$ kN/cm^2, $\rho = 78.5$ kN/m^3). Eurocode 3 design code was used for the dimensioning of the non damped primary frame, resulting in a fundamental period of $T = 0.34$ s and stiffness of $k = 41717.37$ kN/m.

The cables' diameter was kept constant with $d_c = 20$ mm ($E = 1.6 \times 10^4$ kN/cm^2, $f_e = 140$ kN/cm^2) and the resulting bracing stiffness amounts to $k_b = 4191.67$ kN/m. The selection of a single cable's diameter for the analysis follows respective results of a sensitivity analysis that concluded in seismic responses through ADCS with very insignificant differences for $0.05 \leq k_b/k \leq 0.5$ (Phocas and Pocanschi 2003). The cables were assigned a suitable pretension stress and modeled as frame objects with zero compression limit and as cable objects with built-in fuse not to go in compression, representing in both cases the actual behavior of flexible tension-only members. Finally each disc was modeled as a composition of short frame members, assigned with large stiffness values to represent the real property of a shaft supported disc.

3.1 Mechanical properties of hysteretic damper

ADCS may result in significant energy dissipation, when all design parameters involved are predefined respectively for all selected seismic loading cases of the analysis. ADCS response for the desirable level of seismic protection depends primarily on the elastic lateral stiffness of the hysteretic damper, k_d, and the plastic yield force, P_y, of the device, given by the following equations

$$k_d = \frac{n(2 + a/b)EI_b}{h^3} \tag{1}$$

$$P_y = \frac{nf_ybt^2}{6h} \tag{2}$$

where I_b is the elastic moment of inertia at the top section of the steel plates, h is the steel plates' height, b is the lower-width, a is the upper-width, t is the thickness, n is the number of the steel plates and f_y is the yield stress ($S235$, $E = 2.1 \times 10^4$ kN/cm^2, $f_y = 24$ kN/cm^2, $\rho = 78.5$ kN/m^3).

Hysteretic dampers may exhibit a bilinear or trilinear hysteresis, an elasto-plastic or rigid-plastic behavior. The damper used in ADCS was modeled as a non-linear link element, whereas its force-deformation relationship for the respective degree of freedom that corresponds to shear follows the hysteretic model described as Wen plasticity property type of uniaxial deformation (CSI, SAP2000NL 2010).

The damper provides energy dissipation through its hysteretic behavior. Assuming that the kinetic energy of the system is dissipated within the first quarter of the hysteresis loop, the necessary yield force of the damper can be estimated by using the expression

$$E_H = P_yD_d \Rightarrow P_y = \frac{E_H}{D_d} \tag{3}$$

where E_H is the dissipated plastic hysteretic energy, P_y is the plastic yield force of the device and D_d is the damper's shear deformation. A design parameter, defined as damper ratio, DR, that describes

ADCS response as a function of the damper's stiffness and -yield force may be introduced, as follows

$$DR = \frac{k_d}{P_y} \tag{4}$$

For the investigation of the sensitivity of the system's seismic control effectiveness to variations of the characteristic DR parameters, a range of damper's stiffness values of $112\,kN/m < k_d < 24192\,kN/m$ was combined in the analysis with a yield force, varying in the range of $2.60\,kN < P_y < 42.66\,kN$. The geometry of the steel plates was considered to be variable; the height varied between 15-40 cm, the thickness between 0.8-2.0 cm and the number of plates between six to ten. The lower steel plates' width varied between 4-6 cm and the upper steel plates' width was considered to be minimal, 0.5 cm.

3.2 Input seismic records

The primary frame and the controlled system were evaluated in their dynamic behavior under the action of three strong earthquake excitations with differing energy content characteristics, Table 1. The earthquake records represent moderately long, extremely irregular motions. The predominant periods of the ground motions range in their respective displacement response spectra between 1.5-3.0 s. In the analysis no critical damping was considered for the model or the dynamic loading motions.

4. Systems dynamic response

4.1 Natural period

Earthquake resistant systems are characterized at first place by their fundamental period. The period of the controlled system for any DR value is of major importance in ensuring that it doesn't coincide with the prevailing excitation periods, as well as in evaluating possible major differences of the system's response under the selected ground motions. The variation of the controlled system's period in respect to the damper's characteristic parameters, k_d, P_y and DR, is shown in Fig. 4. Compared to the primary frame's fundamental period of $T = 0.34$ s, the controlled system's period decreases slightly to the range of $0.275 < T < 0.28$ s. The controlled system's period results from the two components' stiffness, i.e., the primary frame's- k and the damper's stiffness k_d that are linked in parallel, while substantially remaining independent of P_y (Nakashima, Saburi and Tsuji 1996). The only slight difference within the range of the controlled systems' period allows for the design considerations to be based on the characteristic parameter DR, rather than of T.

Table 1 International seismic input records

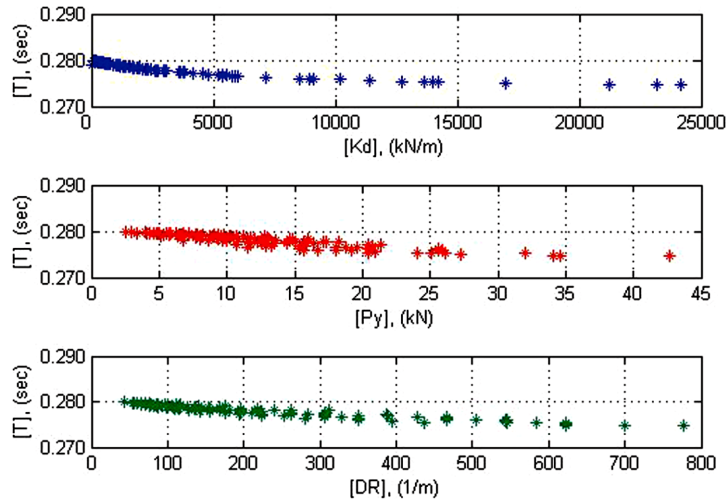| Seismic case	Record	Station	Mw	PGA (g)	Duration (s)
A	El Centro 1940	Imperial valley, component 180	6.9	0.348	53.76
B	Kobe 1995	JMA, component 0	6.9	0.810	48.00
C	Northridge 1994	Olive view, component 90	6.7	0.604	30.00

Fig. 4 Controlled system's fundamental period *T* to damper's stiffness k_{kd}, -yield force P_y and -ratio *DR*

4.2 Energy dissipation

The performance index for structural safety has been defined as effective energy deformation index, EEDI, which physically represents the amount of input seismic energy dissipated by the hysteretic device. A number of 342 combinations of assigned values of the damper's stiffness and yield force in terms of *DR* have been used in the analysis for all seismic loading cases. ADCS energy dissipation function to *DR* is characterized by a power trend line. The ratio values of the hysteretic energy to the input energy of the system are presented in Fig. 5, calculated for each value of *DR*. The energy ratio variation is marked on the *y*-axis and the *x*-axis contains the design parameter *DR*.
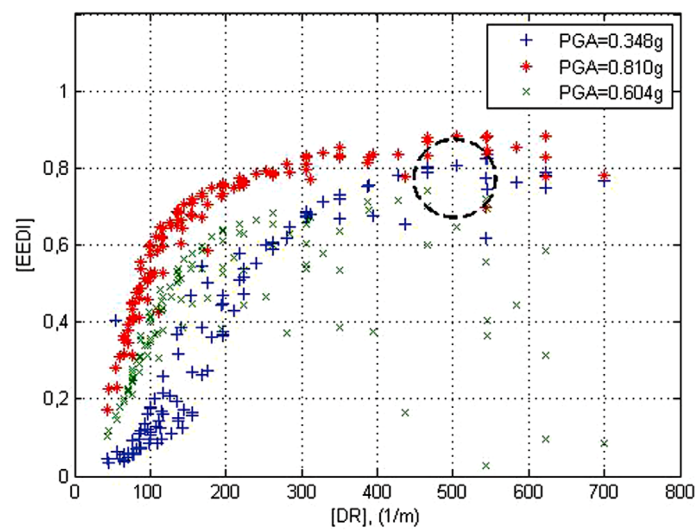

Fig. 5 ADCS effective energy deformation index EEDI to damper ratio *DR*

The selected non-linear parameter, *DR*, proposed to characterize the dynamic response behavior of ADCS, varies between a minimum value of *DR* = 44 1/m and a maximum value of *DR* = 700 1/m. This range of *DR* values shows clearly the predominant characteristic design parameters of ADCS.
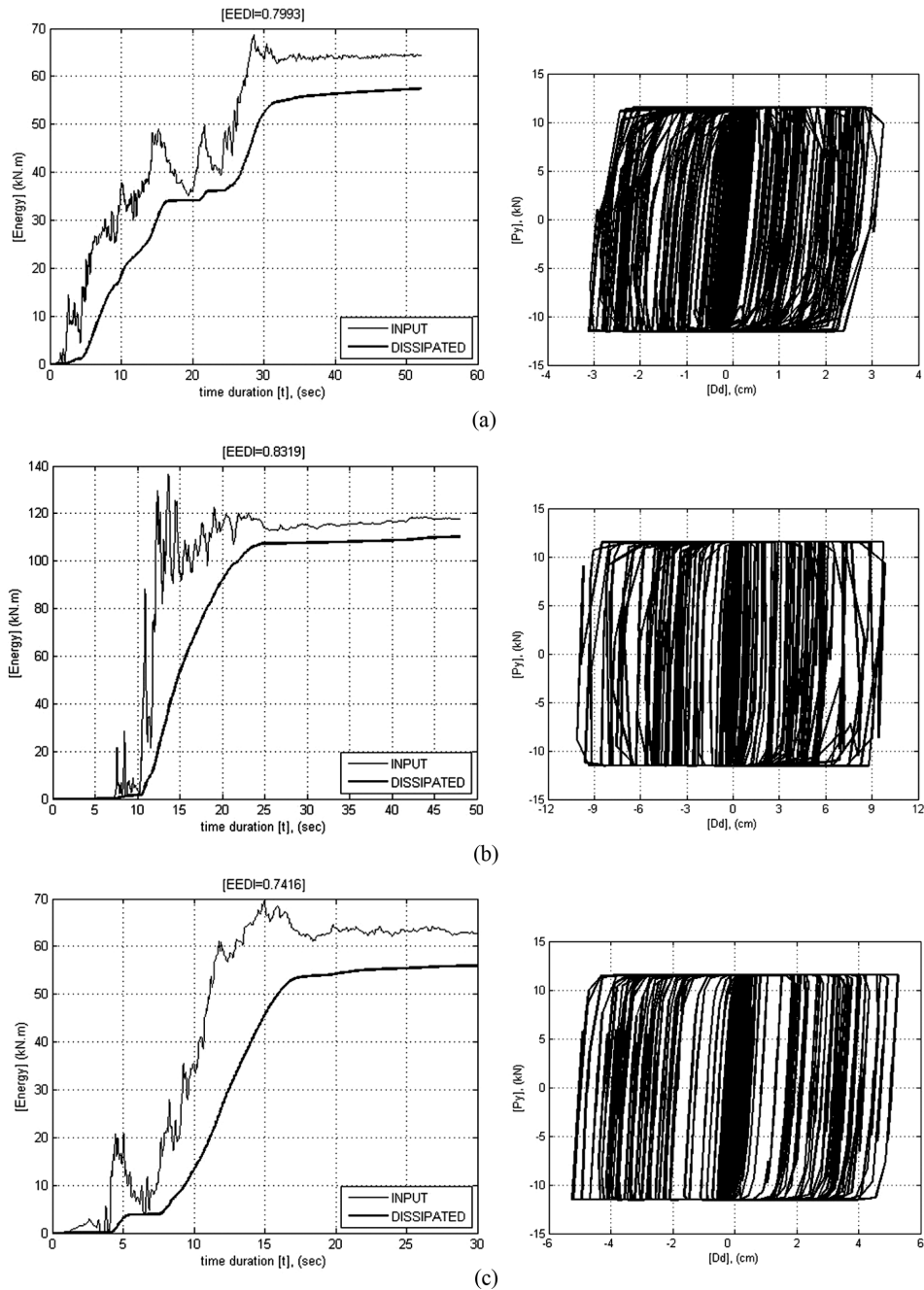

Fig. 6 Hysteretic damper's energy dissipation- and force-deformation behavior (damper: 612155): (a) seismic case A, (b) seismic case B and (c) seismic case C

High energy dissipation by the controlled system, for example exceeding 60% of the input energy, may be achieved for the seismic loading case A with values of $DR > 284$ 1/m. For seismic case B the respective values of DR amount to $DR > 168$ 1/m. In seismic case C the control system may dissipate in only some cases more than 60% of the input energy, when $DR > 200$ 1/m.

Maximum energy dissipation for all three seismic cases are favored by values of $437 < DR < 544$ 1/m, taking into account also reduction of the controlled system's maximum base shear and -relative displacements, as described in the following sections. ADCS energy dissipation is in particular less successful for low values of DR, i.e., $DR < 240$ 1/m, especially for low peak ground accelerations, seismic case A. In the entire DR-range of analysis ADCS performed comparatively better in the seismic case B with highest peak ground acceleration.

The time variations of the system's input- and dissipated energy leading to high energy dissipation performance by ADCS for all three seismic loading cases are shown in Fig. 6. The selected geometry of the damper's steel plates amounts to $n = 6$, $t = 1.2$ cm, $h = 15$ cm and $b = 5$ cm (damper: 612155). The respective optimum DR value amounts to 466.67 1/m ($k_d = 5376$ kN/m, i.e., $k' = k_d/k = 0.129$, $k'' = k_b/k_d = 0.78$, $P_y = 11.52$ kN). EEDI reaches 79.93% in seismic case A, 83.19 % in -case B and 74.16% in -case C. In the parametric study the damper's plates' height, h, proved to influence stronger the system's behavior than the other geometric parameters, b, t and n. The form of the corresponding hysteresis curves depends primarily on the grade of the plastic hysteretic damping. The selected hysteretic damper develops in all three seismic cases exclusively hysteresis curves of the rigid-plastic type model. In these cases the damper determines the dynamic behavior of the system. In addition the hysteretic curves obtained verify an insignificant strength and stiffness deterioration of the damper's plates, which is in support of a stable energy dissipation behavior by the control system.

4.3 Base shear

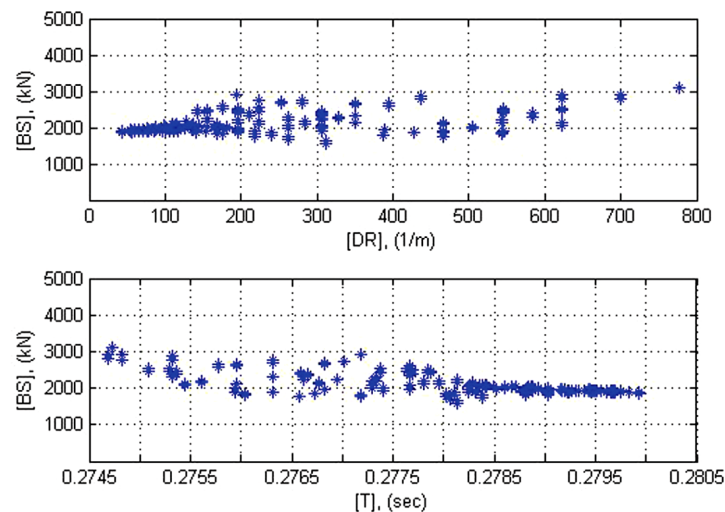ADCS base shear responses under the three strong ground motions used in the analysis indicate

Fig. 7 Controlled system's maximum base shear *BS* to damper ratio *DR* and fundamental period *T* for seismic case A

some basic characteristics of the controlled system's performance. The magnitudes of base shear are presented in absolute values in Figs. 7-9 as a function of DR and T. The parallel presentation of the results in relation to T enables verification of the response relations derived as to DR. The maximum base shear of the controlled systems decreased significantly for the entire DR range of values, compared to the respective primary frame's response, in the seismic loading case B with highest peak ground acceleration. While in seismic case A with lowest peak ground acceleration small reductions of the maximum base shear of the controlled system may be observed especially for low values of DR, i.e., DR < 240 1/m, in seismic case C a considerable increase of the maximum base shear takes place with respective decrease of DR. Even in such cases the controlled
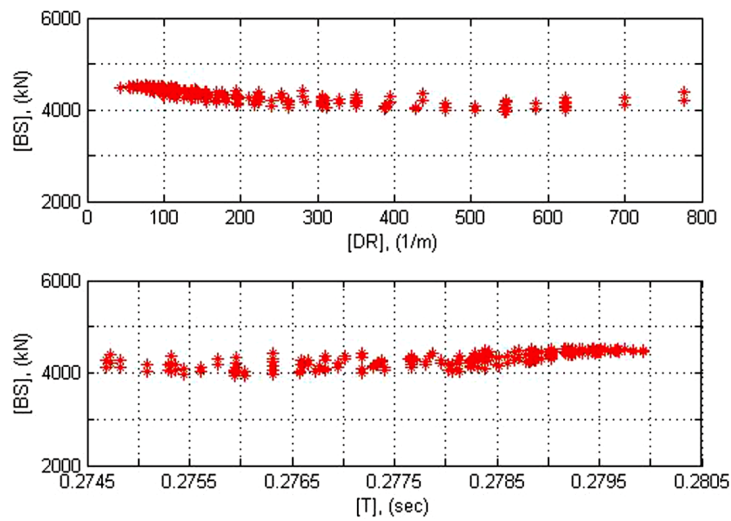

Fig. 8 Controlled system's maximum base shear BS to damper ratio DR and fundamental period T for seismic case B
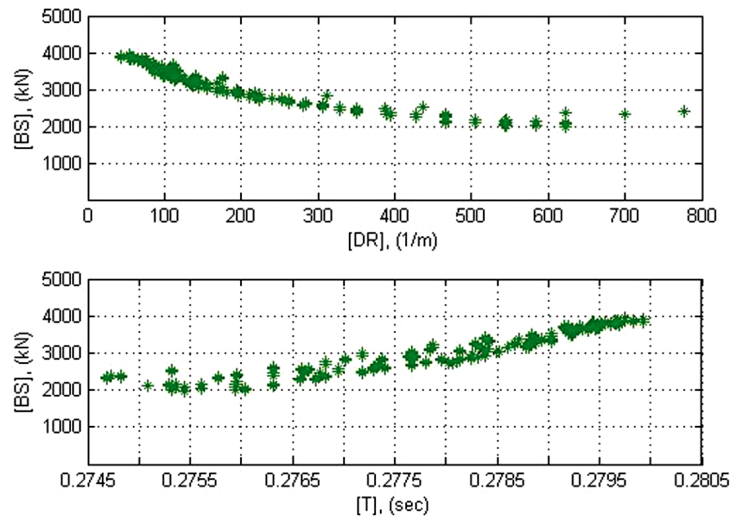

Fig. 9 Controlled system's maximum base shear BS to damper ratio DR and fundamental period T for seismic case C

Table 2 Primary frame's- and ADCS (damper: 612155) base shear response

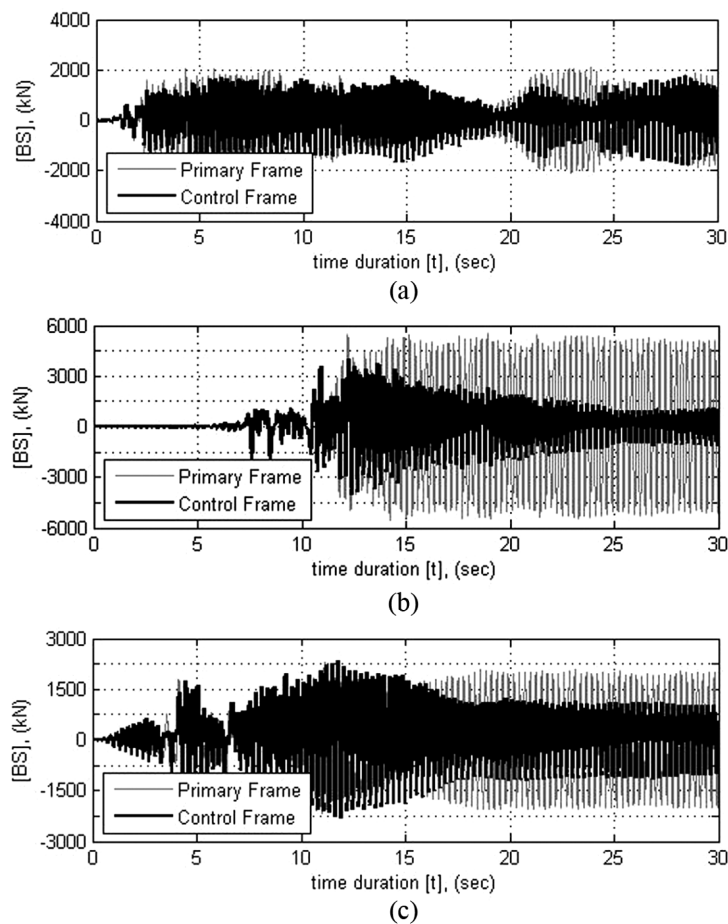| Seismic case	Max. base shear (kN)		Energy dissipation ratio (%)
	Primary frame	ADCS	
A	2102	1764	79.93
B	5570	4031	83.19
C	2304	2321	74.16

Fig. 10 Primary frame's- and controlled system's base shear *BS* - time history (damper: 612155): (a) seismic case A, (b) seismic case B and (c) seismic case C

system's responses did not exceed the limits imposed by the elastic frame design according to Eurocode 3 guidelines.

Within the selected *DR* values for high energy dissipation performance of ADCS, i.e., 437 < *DR* < 544 1/m, the base shear of the controlled systems obtained the lowest values. Compared to the primary frame's base shear, ADCS maximum base shear decreases for a *DR* value of 466.67 1/m (damper: 612155) by 16% in seismic case A, almost by 28% in -case B, whereas in -case C it

increases slightly by 1%, Table 2. In all three cases the energy dissipation effected by ADCS exceeds 74% of the input seismic energy.

Fig. 10 shows the time-history for the first 30 s of the primary frame's base shear (light line) to the controlled system's base shear (dark line) under the three loading cases, for the *DR* value of 466.67 1/m (damper: 612155).

4.4 Relative displacements

The system's relative displacements variation has been investigated for indication of some major trend characteristics in its response behavior. The magnitudes of the system's relative displacements are presented in absolute values in Figs. 11-13 as a function of *DR* and *T*. The minimum response values occur within the range of 437 < *DR* < 544 1/m. The highest responses increase develops with decrease of *DR*, i.e., *DR* < 240 1/m. For all seismic loading cases the system's relative displacements are in agreement with the respective base shear responses. The controlled system's maximum relative displacement decreased significantly for the entire *DR* range of values, compared to the respective primary frame's response, in the seismic loading case B with highest peak ground acceleration, whereas in seismic case C a considerable increase of the maximum relative displacement takes place with a respective decrease of *DR* attaining an upper value of 5.348 cm. The respective most unfavorable responses for seismic case A and -B account to 4.10 cm and 6.131 cm respectively. In this context it may be concluded that the relative displacements of the controlled system increase when the damper initiates the energy dissipation process from early loading stages, i.e., the damper's stiffness k_d is low, while the respective values of P_y, are triggered high, so that maximum resistance is obtained for the purpose of ensuring sufficient cumulative plastic deformation capacity of the damper. This explanation conforms to the system's relative displacement responses as to their period *T*, most clearly indicated in the seismic case B and -C.
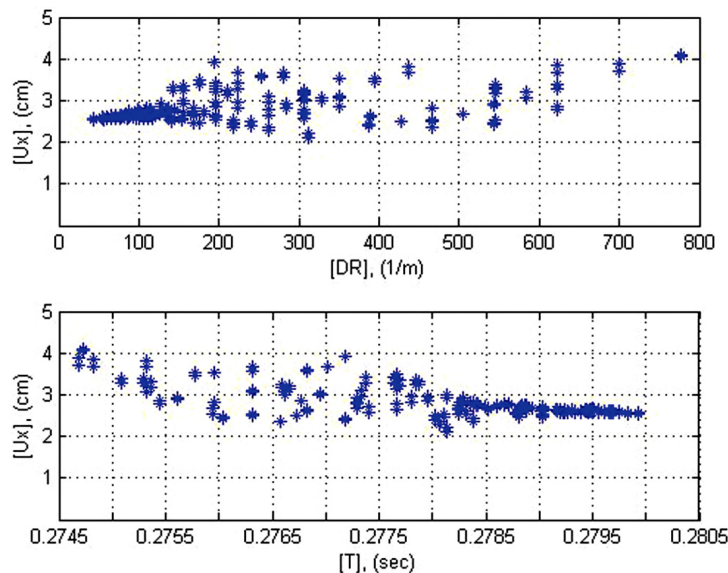

Fig. 11 Controlled system's maximum relative displacements U_x to damper ratio *DR* and fundamental period *T* for seismic case A
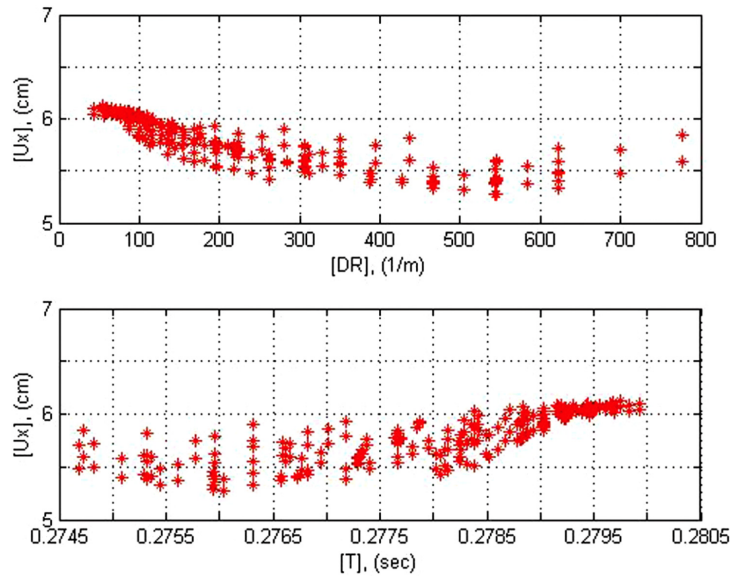
Fig. 12 Controlled system's maximum relative displacements U_x to damper ratio DR and fundamental period T for seismic case B
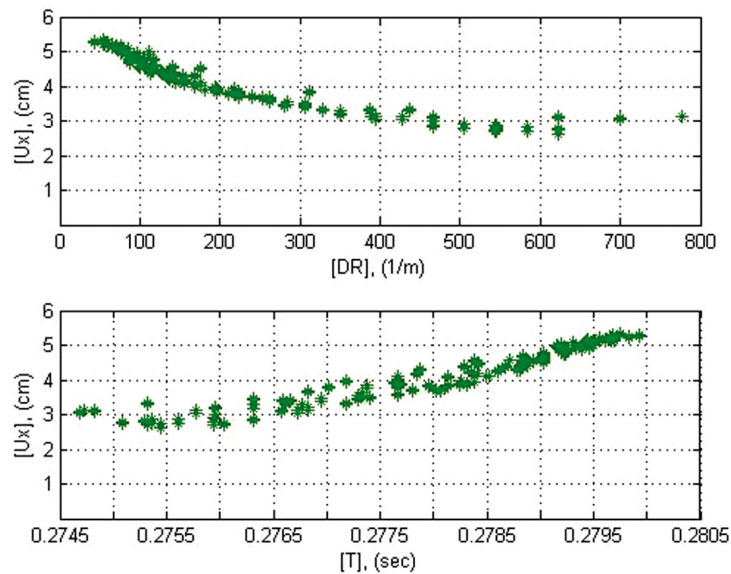

Fig. 13 Controlled system's maximum relative displacements U_x to damper ratio DR and fundamental period T for seismic case C

The reduction of the controlled system's maximum relative displacements compared to the respective values of the primary frame for a DR value of 466.67 1/m (damper: 612155) amounts to approximately 7% for case A and 20% for case B. In the seismic case C the controlled system's maximum relative displacement increased by almost 12% compared to the maximum value of the primary frame, Table 3.

Table 3 Primary frame's- and ADCS (damper: 612155) relative displacements response

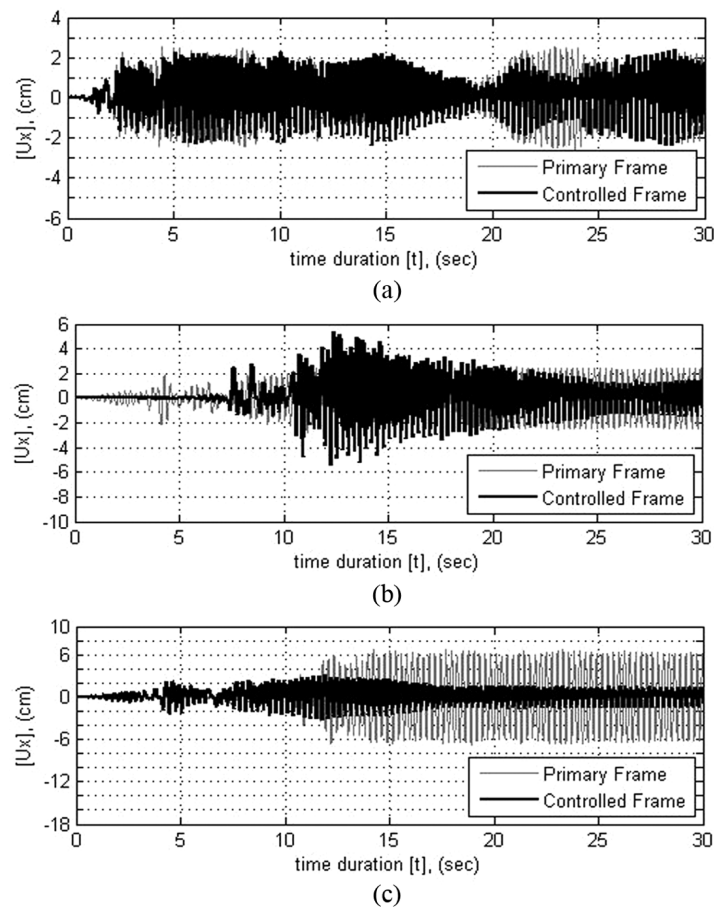| Seismic case	Max. Relative displacement (cm)	
	Primary frame	ADCS
A	2.561	2.372
B	6.779	5.409
C	2.805	3.129

Fig. 14 Primary frame's- and controlled system's relative displacements U_x - time history (damper: 612155): (a) seismic case A, (b) seismic case B and (c) seismic case C

Fig. 14 shows the time-history for the first 30 s of the primary frame's relative displacements (light line) to the controlled system's relative displacements (dark line) under the three loading cases, for the *DR* value of 466.67 1/m (damper: 612155).

4.5 Damper's shear deformations

The hysteretic damper is positioned at the frame's joint area between the secondary bracing
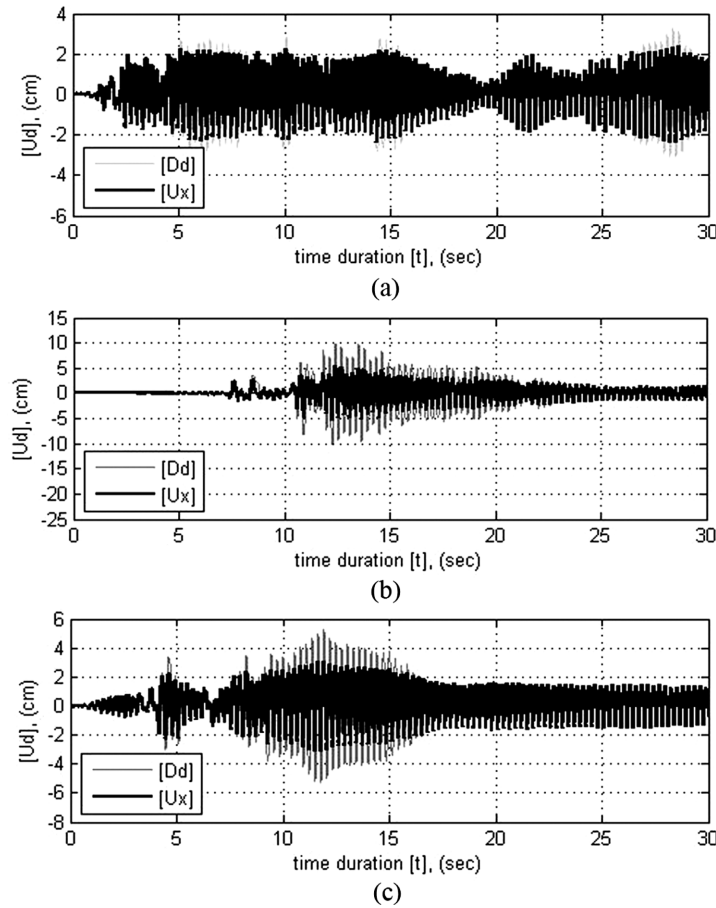
Fig. 15 Damper's shear deformations D_d - and controlled system's relative displacements U_x - time history (damper: 612155): (a) seismic case A, (b) seismic case B and (c) seismic case C

member and the column, so that shear deformations of the device are activated through relative displacements of the primary system to the bracing mechanism. For a *DR* value of 466.67 1/m (damper: 612155), the maximum shear deformations of the damper account to 3.233 cm for seismic case A, 10.25 cm for -case B and 5.244 cm for -case C. Compared to the controlled system's relative displacements the deformation increase of the element accounts to 36.30, 89.50 and 67.59% for the three seismic cases respectively.

Fig. 15 shows the time-history for the first 30 s of the damper's shear deformations for the three loading cases, for a *DR* value of 466.67 1/m (damper: 612155). The light colored lines represent the damper's shear deformations and the dark colored lines, the controlled system's relative displacements.

4.6 Bracings axial force

In the SDOF model the cable bracing was modeled with both, frame- and cable objects, resulting in practically the same response behavior and solved following static nonlinear analysis to represent

Table 4 ADCS cables axial forces (damper: 612155)

Seismic case	Max. tension force (kN)		
	Horizontal member	Diagonal member	Vertical member
A	46.05	72.32	50.46
B	48.56	104.69	59.04
C	47.67	85.84	55.93

the behavior of tension-only bracings for frame objects (zero compression limit) on one hand and of ropes and/or strands for cable objects on the other hand. The static vertical- and horizontal loading of the frame causes tension only to the bracing, whereas under seismic loading also compression develops in the members. A maximum compression force of 63.68 kN was developed in the diagonal bracing member of the controlled system with a *DR* value of 466.67 1/m (damper: 612155), in seismic case B. For this reason, following a trial and error procedure, a prestress of 10% of the maximum allowable stress of the cables' section of $f_e = 140$ kN/cm^2 was applied to the bracing members. In the case of the cables' diameter of $d_c = 20$ mm their respective pretension was set equal to the target force of $F_p = 43.98$ kN. The resulting maximum axial tension forces of the members under the seismic loading cases of the analysis were kept minimum and within the elastic range of deformations, Table 4.

5. Design considerations

Based on the results of the time history analyses a non conservative design approach is suggested for the specific configuration of ADCS presented in the present paper. The design approach refers to strong ground motions of the type "moderately long, extremely irregular motion" and in principle aims at the elastic response of the primary frame under severe earthquake actions. Plastic deformations should only take place in the damping device.

Based on a SDOF model, the design approach consists of the following steps:

1. Establishment of a site-specific design earthquake with 0% of critical damping.
2. Dimensioning of the primary frame structure for static vertical and horizontal loads. The structure should be capable of resisting elastically at least 25% of the static equivalent seismic loads.
   a. Computation of the stiffness of the main structure.
   b. Limitation of the relative displacements of the structure at maximum 1.5% of the height.
3. Determination of the damper's stiffness k_d based on the proposed stiffness factor of the damper's- to the primary frame's stiffness of $k' = 0.129$.
4. Computation of the damper's yield force P_y, according to $DR = 466.67$ 1/m and determination of the damper's plates' dimensions and -number.
   a. The damper's yield force should be higher or equal to 1.5-times the axial diagonal cable force, under wind loading.
5. Computation of the cable bracing's stiffness, according to the stiffness relation of the bracing to the damper, $k'' = 0.78$.
   a. A cables' prestress should ensure that the members develop only tension axial forces during the design earthquake, within their elastic stress limits.

6. Performance of the time history analysis of the structure with the control mechanism under the design earthquake. If necessary, steps 2-6 should be repeated until the individual design criteria are fulfilled.

6. Conclusions

In the present study an adaptable dual control system, ADCS-configuration consisting of a cable bracing - hysteretic damper mechanism, has been introduced and its earthquake responses have been investigated based on a simplified SDOF-model and three international strong ground motions. ADCS enables an interaction free and elastic behavior of the primary structure under static- and severe earthquake loading. ADCS optimization design procedure aiming at highest possible energy dissipation and control of both, base shear and relative displacements of the controlled system, has been performed based on 342 different combinations of characteristic design parameters of the hysteretic damper. An optimum range of damper ratio values has been proposed. For obtaining fitted load-deformation characteristics of the bracing-damper mechanism further experimental investigations are necessary.

References

Chan, R.W. and Albermani, F. (2008), "Experimental study of steel slit damper for passive energy dissipation", *Eng. Struct.*, **30**(4), 1058-1066.

CSI, SAP2000NL. Structural Analysis Programs (2010), *Theoretical and users manual*, Release No. 14.00, Computers & Structures Inc., Berkely, CA.

Dargush, G.F. and Soong, T.T. (1995), "Behavior of metallic plate dampers in seismic passive energy dissipation systems", *Earthq. Spectra*, **11**(4), 545-568.

Di Sarno, L. and Elnashai, A.S. (2005), "Innovative strategies for seismic retrofitting of steel and composite structures", *Progr. Struct. Eng. Mat.*, **7**(3), 115-135.

Filiautrault, A. and Cherry, S. (1988), "Comparative performance of friction damped systems and base isolation systems for earthquake retrofit and aseismic design", *Earthq. Eng. Struct. D.*, **16**(3), 389-416.

Ghabraie, K., Chan, R., Huang, X. and Xie, Y.M. (2010), "Shape optimization of metallic yielding devices for passive mitigation of seismic energy", *Eng. Struct.*, **32**(8), 2258-2267.

Housner, G.W., Bergman, L.A., Caughey, T.K., Chassiakos, A.G., Claus, R.O. and Masri, S.F., Skelton, R.E., Soong, T.T., Spencer, B.F. and Yao, J.P.T. (1997), "Structural control: past, present and future", *J. Eng. Mech.-ASCE*, **123**(9), 897-971.

Kurata, M., DesRoches, R. and Leon, R.T. (2008), "Cable damper bracing for partial seismic rehabilitation", Proceedings of 14th World Conference on Earthquake Engineering, Beijing, China.

Lavan, O. and Levy, R. (2010), "Performance based optimal seismic retrofitting of yielding plane frames using added viscous damping", *Earthq. Struct.*, **1**(3), 307-326.

Li, H.N. and Li, G. (2007), "Experimental study of structure with "dual function" metallic dampers", *Eng. Struct.*, **29**(8), 1917-1928.

Martelli, A. (2007), "Seismic isolation and energy dissipation: worldwide application and perspectives", Brebbia, C.A. (ed.), *Earthquake Resistant Engineering Structures VI*, WIT Press, Southampton, 105-116.

Mualla, I.H. and Belev, B. (2002), "Performance of steel frames with a new friction damper device under earthquake excitation", *Eng. Struct.*, **24**(3), 365-371.

Nakashima, M., Saburi, K. and Tsuji, B. (1996), "Energy input and dissipation behavior of structures with hysteretic dampers", *Earthq. Eng. Struct. D.*, **25**(12), 483-496.

Phocas, M.C. and Pocanschi, A. (2003), "Steel frames with bracing mechanism and hysteretic dampers", *Earthq.*

766 *Marios C. Phocas and Tonia Sophocleous*

Eng. Struct. D., **32**(5), 811-825.
Phocas, M.C. and Sophocleous, T. (2011), "Adaptable dual control systems for earthquake resistance", Brebbia, C.A. and Maugeri, M. (eds.), *Earthquake Resistant Engineering Structures VIII*, WIT Press, Southampton, 55-66.
Renzi, E., Perno, S., Pantanella, S. and Ciampi, V. (2007), "Design, test and analysis of a light-weight dissipative bracing system for seismic protection of structures", *Earthq. Eng. Struct. D.*, **36**(4), 519-539.
Sophocleous, T. and Phocas, M.C. (2011), "Dual structure configuration for earthquake resistance", *Proceedings of the 8th International Conference on Structural Dynamics, EURODYN 2011*, Leuven, Belgium.
Symans, M.D., Charney, F.A., Whittaker, A.S., Constantinou, C., Kircher, C.A. and Johnson, M.W. and McNamara, R.J. (2008), "Energy dissipation systems for seismic applications: current practice and recent developments", *Struct. Eng.*, **134**(1), 3-21.
Tsai, K.C., Chen, H.W., Hong, C.P. and Su, Y.F. (1993), "Design of steel triangular plate energy absorbers for seismic-resistance construction", *Earthq. Spectra*, **9**, 505-528.

SA